25th ABCM International Congress of Mechanical Engineering
October 20-25, 2019, Uberlândia, MG, Brazil

DESIGN AND DEVELOPMENT OF A FIVE-HOLE AERODYNAMIC PROBE

Joel Laguardia Campos Reis
Matheus De Mello Cruz
Guilherme de Souza Papini
Universidade Federal de Minas Gerais – Departamento de Engenharia Mecânica – Av Antonio Carlos, 6627 – Pampulha – Belo Horizonte – Minas Gerais – Brasil, CEP 31.270-901
joellreis@ufmg.br
mmelloc218@yahoo.com
papini@demec.ufmg.br

Abstract. *Development of a reliable instrumentation for the measurement of the airflow characteristics has great importance during a flight test campaign or during wind tunnel tests. The airspeed, static pressure, airflow angles, and other variables must be well known since they are deeply related to the aerodynamic characteristics of an airplane. Among the several types of instruments for this duty, we chose the multi-hole probe as a device for the measurements due to its wide applicability. The aim of this paper is to show the design and development of a five-hole probe that was used to update the flight test platform CEA-FDAS, so that it can generate more reliable data and that can be used for broader operating conditions. The probe was designed based on previous works developed in this laboratory and it was calibrated in a subsonic wind-tunnel to check its accuracy and precision, ensuring its reliability. The developed probe is capable to operate in several flight conditions of a light aircraft and can be used during a certification flight test campaign. Moreover, its operating range can be extended by modifying its pressure sensors or its tip shape. It was designed in such a way that it can be adapted to be used for different scenarios.*

Keywords: *aerodynamic probe, flight test, instrumentation.*

1. INTRODUCTION

The use of reliable instruments for the measurement of the airflow properties in the aerospace industry is of high importance since these quantities are deeply related to several flight characteristics, like stability and control, flight handling qualities, flight performance, and others. The quality of these measurements will directly influence in the data reduction processes used the obtain the aerodynamic characteristics of an aircraft (Jategaonkar, 2006). Among those airflow variables to be measured, we have the airspeed, the airflow direction, the static pressure, the temperature, and others. The Vane Flow Direction Sensor is one of the instruments that can be used to measure the airflow variants. It uses the same principle as that applied in the Pitot-static probe to measure the airflow speed (Anderson, 2007). On the other hand, to measure the airflow directions it uses a system of two vanes, which are connected to potentiometers in such a way that the angles can be correlated to the voltage measured in each of them. One flag is used to measure the airflow angle in the pitch plane and other at the yaw plane, denoted by α and β, respectively.

This is the kind of instrument has been used with the flight data acquisition system (CEA-FDAS) developed in the Center for Aeronautical Studies of the Federal University of Minas Gerais (Oliveira, 2008). However, this instrument has some limitations. Each flag is bi-supported by two mini-bearings which let them spin freely to align with the flow direction, and it can generate difficulties in the developments of this mechanism (Malaquias et al., 2012). Also, during the flag alignment in flight, the inertia of each vane must be accounted to measure the correct airflow direction during the time. Aiming to solve these problems, this paper shows the design and development of a Five-Hole Probe that can be used to make the measurements more reliable for the flight data acquisition system. Moreover, it is shown the aerodynamic analyzes used to determine its design characteristics and also the methodology applied during the calibration phase. This new instrument is more versatile and can also be used for other kinds of tests, like to measure the airflow direction inside a wind tunnel (Wickens and Williams,1985), for the measurement of the skin friction in turbulent flow (Lien and Ahmed, 2011), and others. The Five-Hole Probe is more robust, reliable and suitable for operations in adverse weather conditions (Parameswaran and Jategaonkar, 2004).

2. FIVE-HOLE PROBE PROJECT

The Multi-Hole Probe is a robust instrument for airflow characteristics measurement and is broadly used by the aeronautical industry. Its function principle is based on the pressure difference at different points of the probe when it is subjected to different flow conditions (Jategaonkar, 2006). If we take an axisymmetric probe a larger pressure difference is observed as the angle of incidence is increased, and it is zero when the instrument axis is aligned with the airflow direction (Fig.1).

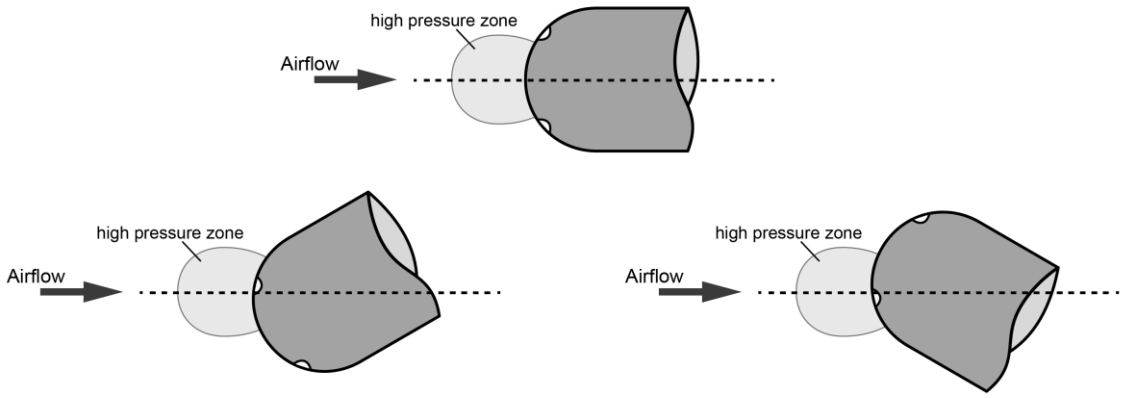

Figure 1. Operation of a Multi-hole Probe

Different tip shapes can be adopted where each of them has a specific sensitivity and linearity level with the change of the airflow incidence angle and speed. Gracey (1958) shows several experimental results obtained for these different tip shapes varying the diameter, airflow regime and orifice angle. It is observed that for subsonic airflow condition, the hemispherical nose shape probe with ½ inch diameter and with the orifices symmetrically separated by 90° is the one with highest sensitivity with the angle of incidence. Since the dynamic pressure also has an influence on the measured value of the angle of incidence, the probe must be able to account for this effect.

The main purpose of this new instrument is to be used with a Flight Test Data Acquisition System (FDAS) that is applied in the development of the airplanes in the Center for Aeronautical Studies of the Federal University of Minas Gerais (CEA-UFMG), where the operational airspeed are between 48 and 210 knots and the angles of attack are generally between -5° and 20°. The probe must also have a good handling property to a fast installation in the airplane and easy storage. Thus, it was chosen to design and build a Five-Hole Probe divided into four parts, since this configuration would be able to measure both the angles on pitch and yaw planes as well as the dynamic pressure in all flight condition, accomplishing with the required handling characteristics. The final design is shown if Fig.2.

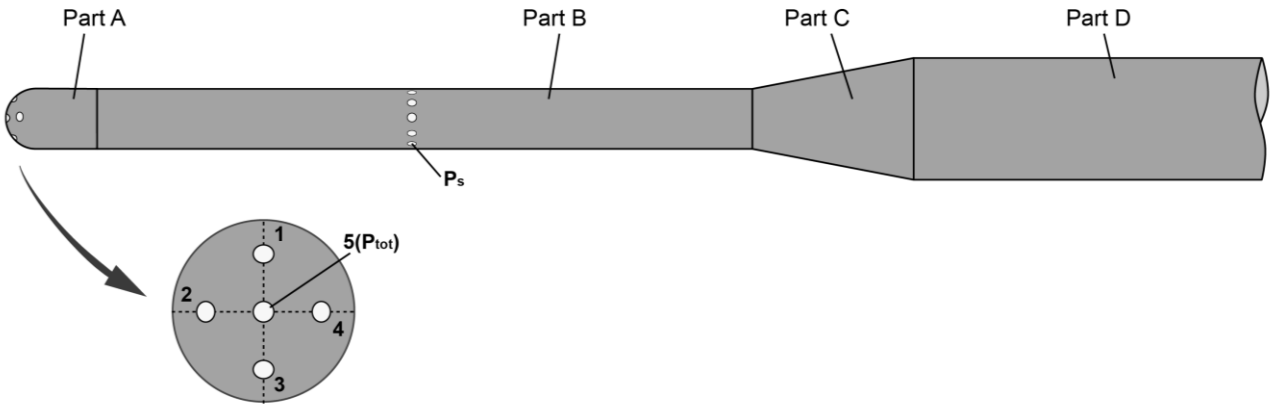

Figure 2. Five-Hole Aerodynamic Probe Project

Part A is the probe tip with five orifices. The central hole measures the total pressure (P_{tot}), and the pressure difference between the holes 1 and 3, and between 2 and 4 is used to correlate with the angle of attack in the pitch plane (α) and with the angle of sideslip in the yaw plane (β), respectively, since:

$$\alpha \propto (\Delta P_{1-3}) \quad (1)$$

$$\beta \propto (\Delta P_{2-4}) \quad (2)$$

The Part B is an elongated tube with an internal isolated chamber where lateral holes are used for the static pressure (P_s) measurement. The frontal pressure orifices are connected to flexible tubes that goes through Part D (Fig.3) and get inside the electronic box, where the pressure sensors are located. The Part D is a 1 inch diameter tube which is used to connect the instrument into the airplane and can be changed to accomplish with the installation requirements shown by McFadden (1952), where a minimal distance from the airplane to the probe tip must be used.

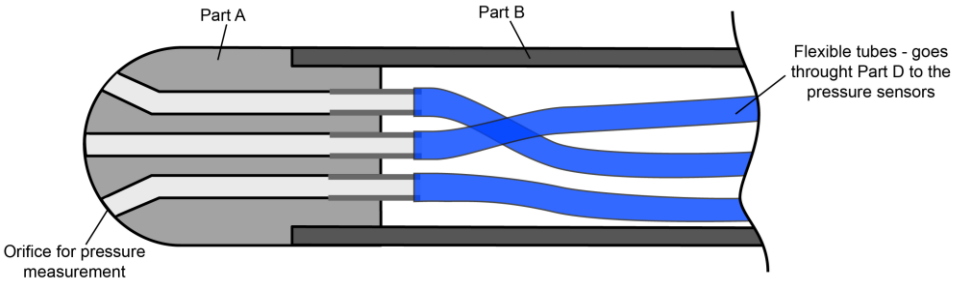

Figure 3. Probe Internal Details

3. CALIBRATION

The experimental analysis of the five-hole probe was done to establish calibration curves for the angles of attack and sideslip and their uncertainty. So, the analysis was divided in the Wind-Tunnel Tests and the Data Reduction.

3.1. Wind-Tunnel Tests

The tests were carried out in the Laboratory of Experimental Aerodynamics of the undergraduate course in aerospace Engineering of UFMG, using the closed-loop wind tunnel, as shown by Figure 4.

The quantities measured were: i) ΔP_{5-s}: the pressure difference between the port 5 and the probe's static ports; ii) ΔP_{2-4}: the pressure difference between ports 2 and 4, on the yaw plane; iii) ΔP_{1-3}: the pressure difference between ports 1 and 3, on the pitch plane; iv) P_s: the absolute value of the flow's static pressure as measured by the probe; v) q_∞: the flow's dynamic pressure, measured by a manometer connected to the tunnel's Pitot-static system, which was held approximately constant through the sampling process; vi) T: the air temperature measured at the beginning of each sampling; vii) the probe's position in reference to the wind-tunnel was read on the rotating table to which the probe's support was attached; and viii) P_{env}: the atmospheric pressure was obtained from the environmental station of the National Meteorology Institute (INMET) located at the Federal University of Minas Gerais (UFMG) . ΔP_{5-s}, ΔP_{2-4}, ΔP_{1-3} and P_s were measured at a sampling rate of 8.6Hz.

These data were acquired at angles and speed conditions expected for a Light Sport Aircraft (LSA) cruise flight. So, speeds of approximately 20m/s, 40m/s and 60m/s and angles between $\pm 20°$ for α and β were chosen. The factors taken into account when deciding the step used in the angle coverage were: i) the uncertainty of the flow direction results can be reduced by calibrating the probe at angles relatively high, as reported by Reichert and Wendt (1994); ii) a finer step should be used when covering the angle interval that most of the cruise flight is expected to take place; and iii) the feasibility and extent of the wind-tunnel test campaign. So, the angles between $-20°$ to $-6°$ and $+6°$ to $+20°$ were measured with a step of 2°, while in between $-5°$ to $+5°$ a 1° step was used. Non-linearities were expected in the resulting calibration curves as the limits of the coverage interval was approached, as a previous pre-calibration showed.

Reynolds numbers covered were 15.000, 30.000 and 45.000, in reference to the probe's diameter. P_{env} and T were used to estimate the freestream density to estimate the Reynolds number.

Regarding the repeatability of the probe's results, 5 samples, composed of around 170 measurements were taken for each orientation, speed and angle set up.

The assessment of the angle α_p between the symmetry line of ports 1 and 3 and the probe's reference line, and its equivalent on the yaw plane, is an indicator of the quality process employed in the probe's construction and should be around 0°. In order to assess its values by the procedure proposed by Clark et al (1992), the measurements were made with the probe on its normal orientation and on its inverted orientation, i.e., rotated $180°$ around its axis. So first the probe was positioned on its support with its pitch plane coinciding with the plane covered by the probe when the wind-tunnel's rotating table was rotated, with a $0°$ sideslip angle. After covering the angular range upwards and downwards, the probe was rotated $180°$ around its axis and the angular range was covered once again upwards and downwards. Afterwards, the

probe was rotated 90° around its axis, so that the yaw plane coincided with the rotation plane, with a 0° angle of attack, and the procedure was repeated. This resulted on independent calibration curves for each angle, an assumption considered reasonable for small angles.

On Figure 4, it is possible to see the probe installed on its support, which is attached to the wind tunnel's rotating table.

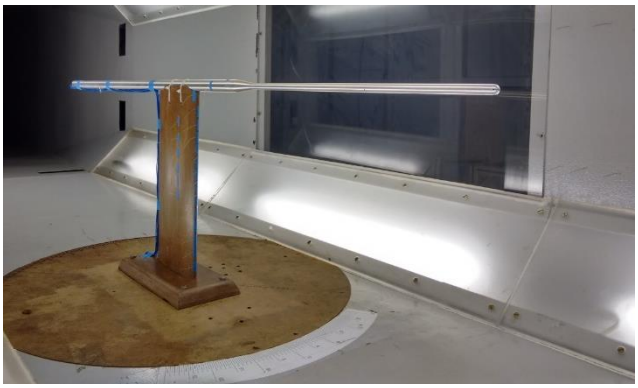

Figure 4. Probe positioned inside wind-tunnel's test section.

3.2. Data Reduction

Only the data reduction process for the angle of attack is presented, as it is analogous for the sideslip angle.

3.2.1. Measurement result

The systematic errors were corrected when evaluating the sample result. By measuring the pressure differences with the wind-tunnel off and the probe positioned at $\alpha = \beta = 0°$, the pressure at all orifices are approximately the same, so the pressure values registered were due to systematic errors and small turbulences inside the wind-tunnel, since the pressure difference should be zero. The latter effect is minimized by measuring the pressure difference on this set up for a relatively long period of time. With this setup, each sample comprised around 1200 measurements. Once the systematic error was known, it could be corrected.

Afterwards, the result of the five samples for each setup were combined to give a result with a lower uncertainty, by use of the standard deviation of the mean. The quantity $\frac{S_P}{\sqrt{N}}$ gives the type A uncertainty of the result for a confidence level of 67% and when multiplied by the value of the t-distribution of 2, since the number N of measurements for each sample was much larger than 30 as recommended by Coleman and Steele (2018), yields the expanded uncertainty $U_x$with a confidence level of 95%. Thus the final result for a test set up was given by Eq. (3).

$$R = R_i \pm U_x = \frac{\sum_{i=1}^{5} \overline{P_i}}{5} \pm t\frac{S_P}{\sqrt{N}} \tag{3}$$

3.2.2. Dynamic Pressure Variation

The pressure difference ΔP_{5-s} approximates well the freestream dynamic pressure for small angles. However, as showed by Pisasale and Ahmed (2002), this approximation becomes jeopardized as the angles of attack and sideslip becomes larger. Thus it was decided to plot the ratio $\Delta P_{5-s}/q_\infty$ throughout the range of angles and speed investigated. Moreover, this analysis showed if there were singularities present, which are encountered when ΔP_{5-s} tends to zero.

3.2.4 Dimensionless Coefficient's Form

A linear fit was made to obtain the calibration curve using four different forms of the dimensionless coefficients, in order to assess the most suitable one. The analysed formulations are presented on Eq. (4) to Eq. (7).

$$c_{p1} = \Delta P_{1-3}/\Delta P_{5-s} \tag{4}$$

$$c_{p2} = \Delta P_{1-3}/q_\infty \tag{5}$$

$$c_{p3} = \Delta P_{1-3}/(\Delta P_{5-s} + P_s) \tag{6}$$

$$c_{p4} = \Delta P_{1-3}/P_s \tag{7}$$

where, c_{p_i} denote the i-th dimensionless pressure coefficient.

The criteria used were: i) a satisfactory angular coefficient at low speeds; ii) lower variation of the angular coefficient of the linear fit through the range of speeds investigated; and iii) the need of flow data external to the probe. The first criterion is due to the lack of sensitivity when the angular coefficient is excessively low, what was seen during a pre-calibration, while the second seeks to minimize the interpolation errors when the speed doesn't match the calibration speeds. Finally, the last criterion is to avoid the need of other instruments, what would increase the cost and the complexity of using the probe.

3.2.5 Calibration Curves

A plot of pressure coefficient versus angle and a linear least-square curve fit of the data was done. This procedure was performed for the probe at its normal and inverted orientation one at a time, as proposed by Clark et al (1992). The linear fits were evaluated at $C_P = 0$ in order to find the angles α_N and α_{Inv}, the angle at which $C_P = 0$ for the normal and the inverted curve respectively. It is important to stress that C_P equals zero when the orifice symmetry axis coincides with the flow direction and this condition doesn't necessarily happens when the probe is at $\alpha = 0°$, because of possible deflections of the flow direction inside the tunnel and due to a deviation of the orifices symmetry axis and the reference axis of the probe that can arise during the manufacturing process.

With α_N and α_{Inv} at hand, it was possible to evaluate α_P and α_f, the flow direction, as proposed by Clark et al (1992). α_f was assumed to be constant throughout the experiment By analysing Figure 5, it is possible to deduce the relations between α_P and α_f for the normal and inverted run, presented on Eq. (8) and Eq. (9), respectively.

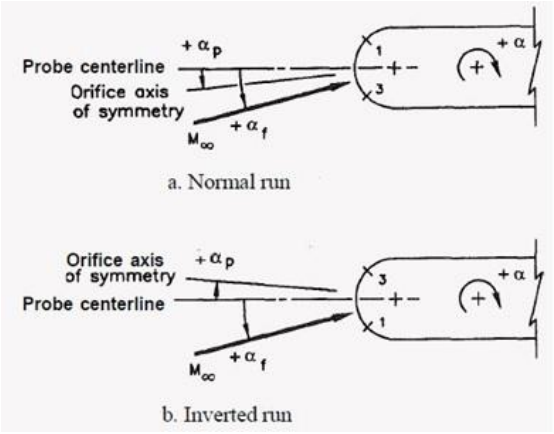

Figure 5. Relations between α_P and α_f. Source: Clark et al (1992), Adapted.

$$\alpha_N = -(\alpha_f - \alpha_p) \tag{8}$$

$$\alpha_{Inv} = -(\alpha_f + \alpha_p) \tag{9}$$

By working with Eq. (8) and (9), one can evaluate α_f, Eq. (10), and α_p, Eq. (11).

$$\alpha_f = -(\alpha_N + \alpha_{Inv})/2 \tag{10}$$

$$\alpha_p = (\alpha_N + \alpha_{Inv})/2 \tag{11}$$

3.2.6 Uncertainty Analysis

The first step in the uncertainty analysis was to calculate the type A uncertainty, as presented on Subsection 3.2.1, of the measurements. With the type A uncertainty of the J parameters involved in the final data reduction equation, one could evaluate the result combined uncertainty u_c, by making use of Eq. (12), as presented by Coleman and Steele (2018):

$$u_c^2 = [\sum_{i=1}^{J} \theta_i^2 b_i^2 + 2\sum_{i=1}^{J-1}\sum_{k=i+1}^{J} \theta_i \theta_k b_{ik} + \sum_{i=1}^{J} \theta_i^2 s_i^2 + 2\sum_{i=1}^{J-1}\sum_{k=i+1}^{J} \theta_i \theta_k s_{ik}] \quad (12)$$

where b_i and s_i are the systematic and random errors, respectively, of the i-th parameter on the result, b_{ik} and s_{ik} are the correlation terms between the systematic errors of the i-th and the k-th parameter and the correlation between the random errors of these parameters, respectively, and $\theta_i = \partial X_r / \partial X_i$ is the coefficient of influence of the i-th parameter on the result X_r.

However, Eq. (12) can be simplified by neglecting the systematic errors, as they were already corrected, and the correlation between the random errors, s_{ik}. This results on Eq. (13).

$$u_c^2 = \sum_{i=1}^{J} \theta_i^2 s_i^2 \quad (13)$$

It is a good practice to analyse the experiment's source of errors, which are thought to be: i) the resolution of the angular marks on the rotating table; ii) probe's misalignment around its own reference axis; iii) support's vibration, mainly at high speed and high angles; iv) probe's weight; v) aerodynamic loading on the probe and its support; vi) temperature and ambient pressure variations; and vii) manufacturing imperfections.

Each of presented errors had an effect on the probe's calibration characteristics. The first source introduced an uncertainty to the positioning of the probe and it is assumed to be $\pm 0.1°$. The second source jeopardized the independence between the yaw and the pitch calibration curves. However, since this misalignment was small, it is not expected that the independency assumption was violated. The third source was expected to cause a greater scatter of the measurements on these conditions. The fourth source caused the fixed angle, while the other one was varying, to be fixed at a value slightly different from $0°$. However, this was not of great influence to the calibration results. The fifth source caused deflections to the probe and its support. The aerodynamic loading on the probe's body were neglected since its project area is relatively small. On the other hand, the torsion of the support was calculated and corrected for, since this would cause a systematic error that would change with the experiment conditions. The sixth source produced a variation of the dynamic and static pressures during the experiments, resulting in a greater scatter of the results. Least, but not last, the seventh source can cause unexpected aerodynamics effects, as the appearance of bubbles or the premature flow separation on the probe's tip.

By normalizing Eq. (13), one can arrive at Eq. (14), where $\frac{u_c}{r}$ and $\frac{U_{X_i}}{X_i}$ are the relative uncertainties of the result and of the i-th parameter. Coleman and Steele (2018) named the term $\left(\frac{X_i}{r}\frac{\partial r}{\partial X_i}\right)$ as Uncertainty Magnifying Factor (UMF) of the i-th parameter and it indicates the influence of this parameter on the final result uncertainty. Thus, during the planning phase of an experiment it is good practice to analyse the UMF of the parameters involved, in order to achieve a satisfactory uncertainty level.

$$\frac{u_c^2}{r^2} = \sum_{i=1}^{J} \left(\frac{X_i}{r}\frac{\partial r}{\partial X_i}\right)^2 \left(\frac{U_{X_i}}{X_i}\right)^2 \quad (14)$$

4. RESULTS AND DISCUSSION

Only the results of the calibration for the pitch plane are presented, since the ones for the yaw plane showed a similar behaviour.

4.1. Dynamic Pressure Variation

The dynamic pressure of 0.2kPa showed the greater data scatter, which decreased with increasing airflow speed. This greater scatter on lower dynamic pressure is most likely to be due not only to the pressure being close to the sensor`s bottom of scale.

The lowering of the dynamic pressure ratio as the angles grow larger corroborate one of the results of Pisasale and Ahmed (2002). Although it was seen that in the range of angles covered on the present paper the ratio doesn't reach zero, what would lead to singularities in the data reduction, greater care should be taken when extrapolating the calibration curves obtained.

4.2. Dimensionless Coefficient's Form

The angular coefficients for Eq. (6) and Eq. (7) showed extremely low values when compared to the ones obtained with Eq. (4) and Eq. (5). So, the former ones didn't satisfy the first criterion. Moreover, both the Eq. (4) and Eq. (5) provided angular coefficients that showed the same behaviour with the variation in airspeed. Thus, the third criterion was used to choose the form presented by Eq. (4), because this formulation didn't use data external to the probe.

4.3. Calibration Curves

The calibration curves were plotted for the speeds analysed and are showed on Figure 6, for $V_\infty = 40\text{m/s}$. By analysing the plots and paying close attention to the data points, it was possible to see that the one-to-one relationship became jeopardized at angles around $\pm 10°$ for $V_\infty = 40\text{m/s}$ and $\pm 15°$ for $V_\infty = 60\text{m/s}$, while for V_∞= 20m/s even at around smaller angles this condition was already compromised. Moreover, it was possible to see that the behaviour of the data points at higher angles, lowered the quality of the fit at small angles, where an almost linear relation between angle and pressure coefficient was seen. Thus it was decided to limit the probe angular range to $\pm 10°$ and redo the plots.

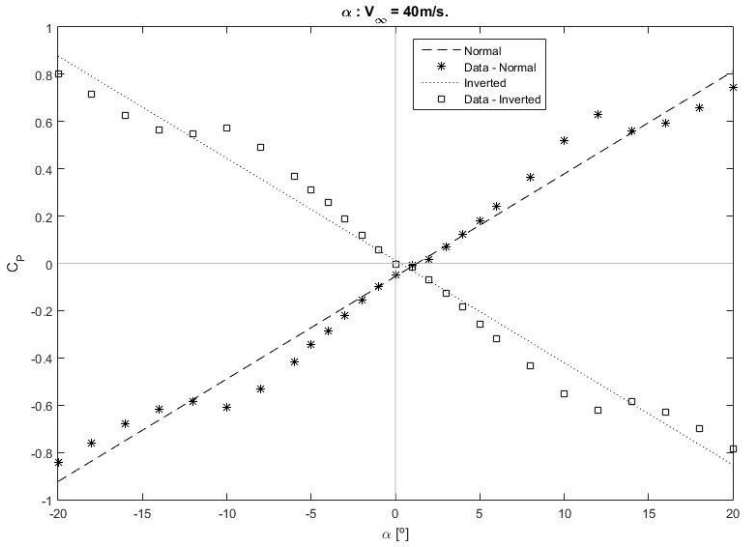

Figure 6. Calibration curves for α at $V_\infty = 40\text{m/s}$ over $\pm 20°$.

The calibration curves over a narrower range are plotted on Figure 7. By comparison of the previous curves with the limited ones, it is possible to see that quality of the fit for small angles is improved as can be seen by the lower deviation of the data points to the linear fit. However, as for $V_\infty = 20\text{m/s}$ the one-to-one relationship was already jeopardized around $0°$, it indicated that the speed range should also be limited.

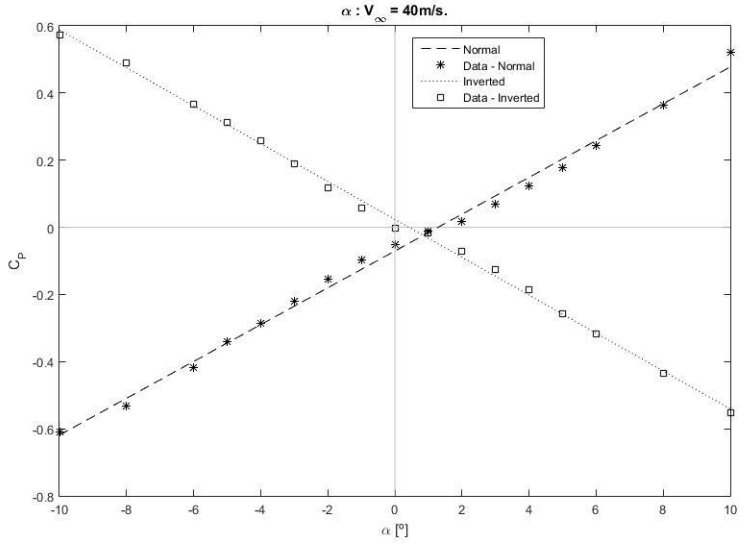

Figure 7. Calibration curves for α at $V_\infty = 40\text{m/s}$ over $\pm 10°$.

With the limited curve fit, it was possible to be more confident on the values of α_f and α_p obtained, which are presented on Table 1. It was seen that the flow direction and the angular deviation between the orifice symmetry axis and the probe's reference axis stabilized at 40m/s and higher speeds, within a 0.03° tolerance on the pitch plane. The great difference between the values for α_p for 20m/s and the other speeds was another sign of that the probe's speed range should be limited, since this is geometric property of the probe. The variation of α_p is believed to be due to the uncertainty of the measurements.

Table 1. Flow direction and deviation angle between the orifice symmetry axis and the probe's reference axis.

Plane	Speed [m/s]	α_f	α_p
Pitch Plane	20	1,12º	-1,34º
	40	0,43 º	-0,85 º
	60	0,46 º	-0,83 º

4.4. Uncertainty Analysis

Since, during the determination of the angle, the calculated pressure coefficient is an input, it was decided to plot curves where the coefficient was on the abscissa axis and the angles on the ordinated. This was done by rearranging the linear fit to Eq. (15), where A_1 is the linear term and A_0 is the independent one. Afterwards, Eq. (13) was used to propagate the random errors of Δp and Δp_{ts} to the result of Eq. (15).

$$\alpha = \frac{C_P}{A_1} - \frac{A_0}{A_1} = \frac{1}{A_1}\frac{\Delta p}{\Delta p_{ts}} - \frac{A_0}{A_1} \tag{15}$$

On Figure 8, one can see the resulting calibration curves with correction for the flow direction, torsion of the support and inaccuracy caused by the rotating table marks. Also the linear fits and the uncertainty of the angles for a confidence level of 95% were plotted as well. On Table 2, one can the result of the uncertainty analysis, consisting of the highest and the lowest uncertainties as well as the UPC of the highest uncertainty. Finally, on Fig. 9 one can the result of the UMF analysis.

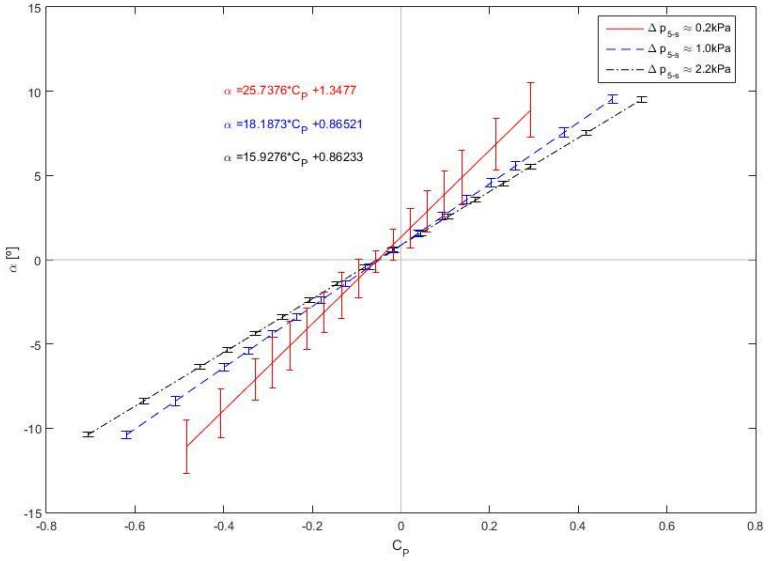

Figure 8. Calibration curves corrected for flow direction, support's torsion and rotating table marks.

Table 2. Flow direction uncertainty analysis.

Plane	Speed [m/s]	U_{max}	U_{min}
Pitch Plane	20	1,64º	0,66º
	40	0,26 º	0,16º
	60	0,16 º	0,12º

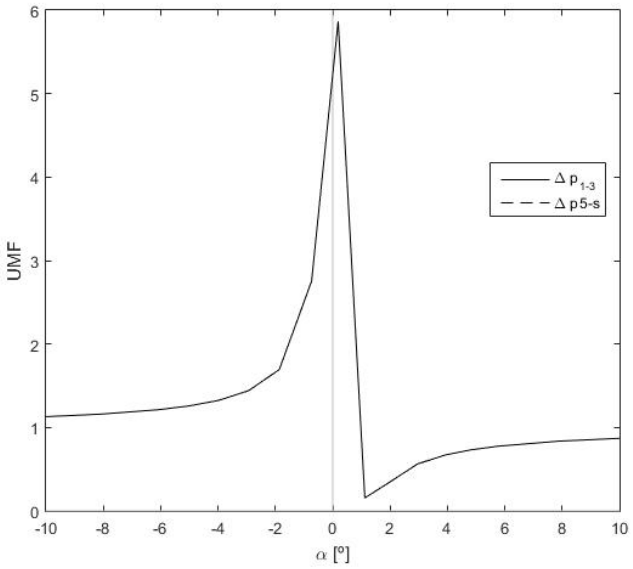

Figure 9. UMF Analysis.

5. CONCLUSIONS

The probe calibration demonstrate it is suitable to be used experimentally, although its limitations suggest that it is more adequate to tests where small angles of attack and sideslip are expected and the speeds are not too low, such as cruise performance test and the assessment of the flow direction in a wind-tunnel.

It was possible to reproduce the P_{5-s} behaviour presented by Pisasale and Ahmed (2002), which conclude that this pressure is indeed a good approximation of the flow dynamic pressure at lower angles, but as the angle increases this approximation becomes jeopardized. Thus, greater care should be taken when extrapolating the dynamic pressure.

The probe's calibration results showed a great variation not only with the airspeed, but with the airflow direction as well. Firstly, the uncertainty was larger for higher angles. Secondly, while the uncertainty can be acceptable at higher speeds, at lower speeds efforts should be made in order to reduce it, such as the use of multiple sensors. Also, a more extensive calibration campaign can be beneficial in this sense.

The wind tunnel's flow direction for the conditions analysed were also evaluated. A greater deflection of the flow was seen at lower speeds and this deflection seems to stabilize from 40m/s on, for the conditions investigated.

6. REFERENCES

Anderson, J., 2007. *Fundamentals of Aerodynamics.* McGraw-Hill, New York, 5th edition.

Clark, E. L.; Henfling, J. F.; Aeschliman, D. P., 1992. "Calibration of Hemispherical-Head Flow Angularity Probes". AIAA 17th Aerospace Ground Testing Conference.

Coleman, H. W., Steele, W. G., 2018. *Experimentation, Validation, and Uncertainty Analysis for Engineers*. John Wiley & Sons, 4th Edition.

Gracey, M.,1958 "Summary of Methods of Measuring Angle of Attack on Aircraft". NACA Technical Note 4351. Washington.

Jategaonkar, R.V., 2006. *Flight Vehicle System Identification: A Time Domain Methodology*. American Institute of Aeronautics and Astronautics Inc, Reston, 1st edition.

Lien, S.J., Ahmed, N.A., 2011. "An examination of suitability of multi-hole pressure probe technique for skin friction measurement in turbulent flow". *Flow Measurement and Instrumentations*, Vol. 5, pp. 153-164.

Malaquias, I.M., da Silva Filho, A.R., Oliveira, P.H.I.A., Thums, G.D., 2012. "Design and Development of a Wireless Pitot Tube for Utilization in Flight Test". *In Proceedings of the 21th International Confress of Mechanical Engineering – COBEM 2011*. Natal, Brazil.

McFadden, N. M., Holden, G. R., Ratcliff, J. W., 1952. "Instrumentation and Calibration Techniques for Flight Calibration of Angle-of-Attack Systems on Aircraft". NACA Research Memorandum A521I23.

Oliveira, P.H.I.A., 2008. "Low-cost Flight Test System for Light Aircrafts". *Aircraft Engineering and Aerospace Technology: An International ounrla. Emerald Group Publishing Limited*.

Parameswaran, V., Jategaonkar, R.V., 2004. “Calibration of 5-hole Probe for Flow Angles from Advanced Technologies

Pisasale, A. J., Ahmed, N. A., 2002. “A novel method for extending the calibration range of five-hole probe for highly three-dimensional flows”. *Flow Measurement and Instrumentations,* Vol. 13, pp. 23-30.

Reichert, B. A., Wendt, B. J., 1994 “A New Algorithm for Five-Hole Probe Calibration, Data Reduction, and Uncertainty Analysis”. NASA Technical Memorandum 106458.

Testing Aircraft System Flight Data”. *Deference Science Journal,* Vol. 54, No. 2, pp. 111-123.

Wickens, R.H., Williams, C.D., 1985. “Calibration and use of Five-Hole Flow Directions Probes for Low Speed Wind Tunnel Application”. Aeronautical Note NAE-AN-29. Otawa, USA.

7. RESPONSIBILITY NOTICE

The authors are the only responsible for the printed material included in this paper.